Nonlinear Dyn (2007) 50:639–650
DOI 10.1007/s11071-006-9185-y

ORIGINAL ARTICLE

Sub-harmonic resonance in a nearly pre-loaded mechanical oscillator

Chengwu Duan · Todd E. Rook · Rajendra Singh

Received: 7 February 2006 / Accepted: 11 November 2006 / Published online: 12 January 2007

Abstract In this paper, the sub-harmonic resonance of a single degree of freedom system with a nearly preloaded non-linearity (gain-changing clearance) is studied. First, a new perturbation approach is incorporated in the traditional multi-term harmonic balance method to calculate the sub-harmonic resonance. Our approach significantly reduces the work as it computes the sub-harmonic responses with just one run. Initial guesses in the vicinity of sub-harmonic regime are relaxed compared to prior approaches. Second, a parametric study is conducted to examine the occurrence and characteristics of sub-harmonic resonance. The possibility of the sub-harmonic occurrence increases with an increase of dynamic excitation or the stiffness ratio. For instance, our analysis shows that the sub-harmonic resonance typically occurs when the mean load is close to the stiffness transition point. In the extreme case, a very small excitation would generate a sub-harmonic resonance. With a higher mean load, the resonant peak appears at lower frequencies as a result of the reduced equivalent stiffness. Finally, our analytical formulation is successfully validated using numerical integration results.

C. Duan · T. E. Rook · R. Singh (✉)
Acoustics and Dynamics Laboratory, Department of Mechanical Engineering and The Center for Automotive Research, The Ohio State University, 201 West 19th Avenue, Columbus, OH 43210, USA
e-mail: singh.3@osu.edu

Keywords Sub-harmonic resonance · Mechanical oscillator · Discontinuous non-linearity

Abbreviations

MHBM	multi-term harmonic balance method
max	maximum value
min	minimum value
rms	root mean square

1 Introduction

Mechanical oscillators with dual-staged piecewise linear stiffness characteristics (as shown in Fig. 1) have received considerable inquiry since their dynamic responses exhibit strong nonlinear characteristics depending on the mean and dynamic loads [1–7]. Taking α as the ratio of first and second stage stiffness elements, one could study various cases of α. Geometrically, two extreme cases of α exist: (i) $\alpha = 0$ for the gap or backlash element and (ii) $\alpha = \infty$ for the "true" preload case. When the system degenerates from nonlinear to linear ($\alpha = 1.0$) case from two extreme ends, the in-between regimes are categorized as the clearance non-linearity ($0 \leq \alpha < 1.0$) and nearly pre-loaded non-linearity ($1.0 < \alpha < \infty$). However, much attention has focused on the backlash or gap non-linearity or on the clearance non-linearity case. For instance, Padmanabhan and Singh [3, 4] examined the nonlinear frequency responses of a gear pair with backlash. Kim et al. [5] further extended the specific gear pair

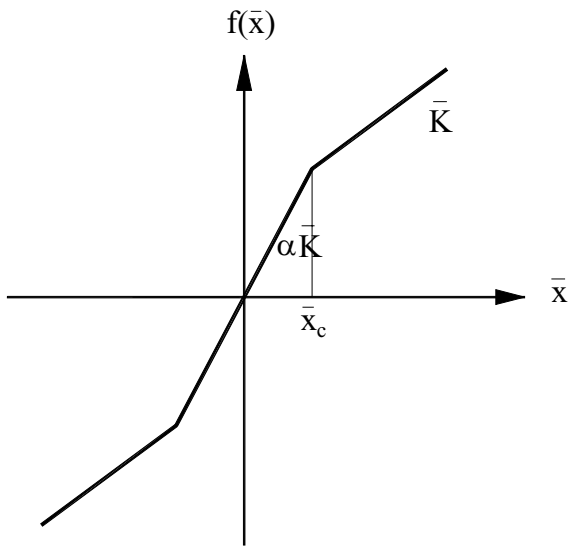

Fig. 1 Nearly pre-loaded non-linearity with α between 1.0 and ∞

formulation to a more general problem. In a recent paper, Duan and Singh [6] studied the $\alpha = \infty$ case. Further, super-harmonic resonances have been examined (primarily for the case when α varies between 0 and 1.0), as evident from the work of Kim et al. [5] and Padmanabhan and Singh [4]. Yet, it seems that the nearly pre-loaded case, when α varies between 1.0 and ∞, has not received much attention. Gelb and Vander Velde [7] have defined this as a "gain-changing" non-linearity and have provided a solution at the primary harmonic by employing the well-known describing function method. But, sub-harmonics in such a system have never been examined though Padmanabhan and Singh [6] investigated them for $\alpha = 0$ case. Therefore, the chief goal of this paper is to analytically and computationally examine sub-harmonic responses, for the mechanical oscillator with α greater than 1.0.

2 Problem formulation

Consider a single degree of freedom system with mass $\bar{M}$, viscous damping $\bar{C}$ and piece-wise linear function $f(\bar{x})$ (of Fig. 1) where $\bar{K}$ is the second stage stiffness. Further, apply the mean load $\bar{F}_\mathrm{m}$ and harmonic force of amplitude $\bar{F}_\mathrm{p}$ as shown below where $\dot{\bar{x}} = d\bar{x}/d\bar{t}$.

$$\bar{M}\ddot{\bar{x}} + \bar{C}\dot{\bar{x}} + \bar{K}f(\bar{x}) = \bar{F}_\mathrm{m} + \bar{F}_\mathrm{p}\sin(\bar{\omega}\bar{t}) \tag{1}$$

and,

$$f(\bar{x}) = \left\{ \begin{matrix} \bar{x} - (1-\alpha)\bar{x}_\mathrm{c} & \bar{x} > \bar{x}_\mathrm{c} \\ \alpha\bar{x} & |\bar{x}| \le \bar{x}_\mathrm{c} \\ \bar{x} + (1-\alpha)\bar{x}_\mathrm{c} & \bar{x} < -\bar{x}_\mathrm{c} \end{matrix} \right\}, \alpha \in (1, \infty) \tag{2a}$$

Rewrite the above in a compact form as,

$$f(\bar{x}) = \bar{x} + \left(\frac{1-\alpha}{2}\right)[|\bar{x} - \bar{x}_\mathrm{c}| - |\bar{x} + \bar{x}_\mathrm{c}|] \tag{2b}$$

$$f(\bar{x}) = \bar{x} + (1-\alpha) \times \frac{(\bar{x} - \bar{x}_\mathrm{c})\mathrm{sgn}(\bar{x} - \bar{x}_\mathrm{c}) - (\bar{x} + \bar{x}_\mathrm{c})\mathrm{sgn}(\bar{x} + \bar{x}_\mathrm{c})}{2} \tag{2c}$$

Here, sgn(·) is the triple-valued signum function. Further, Equation (1) is non-dimensionalized by introducing the following dimensionless parameters and taking $\alpha\bar{x}_\mathrm{c}$ as characteristic displacement.

$$\bar{\omega}_\mathrm{n} = \sqrt{\bar{K}/\bar{M}}, \tag{3a}$$

$$\Omega = \bar{\omega}/\bar{\omega}_\mathrm{n}, \tag{3b}$$

$$\tau = \bar{\omega}_\mathrm{n}\bar{t}, \tag{3c}$$

$$x = \bar{x}/(\alpha\bar{x}_\mathrm{c}), \tag{3d}$$

$$\varsigma = \bar{C}/2\sqrt{\bar{K}\bar{M}}, \tag{3e}$$

$$F_\mathrm{m} = \bar{F}_\mathrm{m}/(\bar{K}\alpha\bar{x}_\mathrm{c}), \tag{3f}$$

$$F_\mathrm{p} = \bar{F}_\mathrm{p}/(\bar{K}\alpha\bar{x}_\mathrm{c}). \tag{3g}$$

Thus, we obtain the governing equation in the following form where $()'$ represents $d()'/d\tau$.

$$x'' + 2\varsigma x' + f(x) = F_\mathrm{m} + F_\mathrm{p}\sin(\Omega\tau) \tag{4}$$

By choosing $\alpha\bar{x}_\mathrm{c}$ as characteristic displacement (assuming that α is not infinity), the initial operating point can be easily identified since $F_\mathrm{m} = 1.0$ would exactly correspond to the transition from the first to the second stage. A new perturbation approach will be introduced in this article for the calculation of sub-harmonics when α varies between 1 and ∞. In particular, effects of F_m, F_p and α on the occurrence of sub-harmonic resonances will be investigated. We will however focus on the second sub-harmonic resonance for the sake of brevity.

Finally our analytical formulation will be validated using numerical solutions.

3 Calculation of sub-harmonic resonance

3.1 Multi-term harmonic balance method

Multi-term harmonic balance method (MHBM) has been widely used for nonlinear problem. For instance, refer to [5] for detailed mathematical formulation. Recently, Duan and Singh [6] developed an indirect MHBM for the pre-load type non-linearity when $\alpha = \infty$. The fundamental principle of HBM is to represent periodic excitation and response by a truncated harmonic series, as shown below; refer to the list of symbols (Appendix A) for the identification of symbols.

$$x(\tau) = a_o + \sum_{n=1}^{N_h \upsilon} a_{2n-1} \sin\left(\frac{n}{\upsilon}\Omega\tau\right) + a_{2n} \cos\left(\frac{n}{\upsilon}\Omega\tau\right). \tag{5a}$$

$$f(x(\tau)) = c_o + \sum_{n=1}^{N_h \upsilon} c_{2n-1} \sin\left(\frac{n}{\upsilon}\Omega\tau\right) + c_{2n} \cos\left(\frac{n}{\upsilon}\Omega\tau\right). \tag{5b}$$

$$F(\tau) = q_0 + \sum_{m=1}^{N_h} q_{2m-1} \sin(m\Omega\tau) + q_{2m} \cos(m\Omega\tau) \tag{5c}$$

Or in discrete matrix form,

$$\left(\frac{\Omega}{\upsilon}\right)^2 \underline{\underline{\mathbf{\Gamma\Delta}}}^2 \underline{\mathbf{a}} + 2\varsigma \left(\frac{\Omega}{\upsilon}\right) \underline{\underline{\mathbf{\Gamma\Delta}}}\,\underline{\mathbf{a}} + \underline{\underline{\Gamma}}\,\underline{\mathbf{c}} = \underline{\underline{\Gamma}}\,\underline{\mathbf{Q}} \tag{6}$$

Here $\underline{\underline{\mathbf{\Gamma}}}$ is an operator digitizing the continuous data, $\underline{\underline{\mathbf{\Delta}}}$ is to perform derivation function, $\underline{\mathbf{a}}$ is Fourier coefficients of nonlinear response $x(\tau)$, $\underline{\mathbf{c}}$ is coefficients for $f(x(\tau))$, $\underline{\mathbf{Q}}$ contains coefficients of excitation.

$$\underline{\underline{\mathbf{\Gamma}}} = \begin{bmatrix} 1 & \sin\left(\frac{\Omega}{\upsilon}\tau_0\right) & \cos\left(\frac{\Omega}{\upsilon}\tau_0\right) & \sin\left(\frac{2\Omega}{\upsilon}\tau_0\right) & \cdots & \cos\left(\frac{N_h\upsilon\Omega}{\upsilon}\tau_0\right) \\ 1 & \sin\left(\frac{\Omega}{\upsilon}\tau_1\right) & \cos\left(\frac{\Omega}{\upsilon}\tau_1\right) & \sin\left(\frac{2\Omega}{\upsilon}\tau_1\right) & \cdots & \cos\left(\frac{N_h\upsilon\Omega}{\upsilon}\tau_1\right) \\ \vdots & \vdots & \vdots & \vdots & \vdots & \vdots \\ 1 & \sin\left(\frac{\Omega}{\upsilon}\tau_{N-1}\right) & \cos\left(\frac{\Omega}{\upsilon}\tau_{N-1}\right) & \sin\left(\frac{2\Omega}{\upsilon}\tau_{N-1}\right) & \cdots & \cos\left(\frac{N_h\upsilon\Omega}{\upsilon}\tau_{N-1}\right) \end{bmatrix}, \tag{7a}$$

$$\underline{\underline{\mathbf{\Delta}}} = \begin{bmatrix} 0 & & & \\ & \begin{bmatrix} 0 & 1 \\ -1 & 0 \end{bmatrix} & & \\ & & \ddots & \\ & & & \begin{bmatrix} 0 & N_h\upsilon \\ -N_h\upsilon & 0 \end{bmatrix} \end{bmatrix}. \tag{7b}$$

and υ is sub-harmonic index. In the case when the second sub-harmonics are sought, $\upsilon = 2$. Further, since excitation is known, $\underline{\mathbf{Q}}$ is written as:

$$\underline{\mathbf{Q}} = [\,F_{\mathrm{m}} |\quad 0 \quad 0 |\quad F_{\mathrm{p}} \quad 0 |\quad \cdots \quad |0 \quad 0\,]^T \tag{8}$$

Here F_{p} is 2υth element of the input vector. By introducing a pseudo inverse of $\underline{\underline{\mathbf{\Gamma}}}^+ = (\underline{\underline{\mathbf{\Gamma}}}^T\underline{\underline{\mathbf{\Gamma}}})^{-1}\underline{\underline{\mathbf{\Gamma}}}^T$, we obtain the following residual that is to be minimized:

$$\underline{\mathbf{\Theta}}(\underline{\mathbf{a}}, \Omega) = \left(\frac{\Omega}{\upsilon}\right)^2 \underline{\underline{\mathbf{\Delta}}}^2\underline{\mathbf{a}} + 2\varsigma\left(\frac{\Omega}{\upsilon}\right)\underline{\underline{\mathbf{\Delta}}}\,\underline{\mathbf{a}} + \underline{\mathbf{c}} - \underline{\mathbf{Q}} \tag{9}$$

The coefficients $\underline{\mathbf{a}}$ can be obtained through a Newton–Raphson iteration scheme from a certain starting point Ω_0 and initial guess of $\underline{\mathbf{a_0}}$. A frequency sweep can be conducted by implementing a continuation scheme in conjunction with the Newton–Raphson iteration. Subsequently, the stability of the converged periodic responses can be determined by Hill's method as in [5]. This particular method would work fine for the limiting case when $0 \le \alpha \le 1$. Conversely when $\alpha \gg 1.0$, we will encounter numerical stiffness problem as a result of poor-conditioned Jacobian contributed by $\partial \underline{f}/\partial \underline{x}$ in a manner similar to the pre-loaded problem [6].

$$\underline{\underline{\mathbf{J}}} = \frac{\partial \underline{\Theta}}{\partial \underline{\mathbf{a}}} = \left(\frac{\Omega}{\upsilon}\right)^2 \underline{\underline{\mathbf{\Delta}}}^2 + 2\varsigma\left(\frac{\Omega}{\upsilon}\right)\underline{\underline{\mathbf{\Delta}}} + \frac{\partial \underline{c}}{\partial \underline{\mathbf{a}}} \tag{10a}$$

$$\frac{\partial \underline{\mathbf{c}}}{\partial \underline{\mathbf{a}}} = \underline{\underline{\mathbf{\Gamma}}}^+ \frac{\partial \underline{\mathbf{f}}}{\partial \underline{\mathbf{x}}} \underline{\underline{\mathbf{\Gamma}}} \tag{10b}$$

In indirect MHBM [6], the force-displacement relationship in Fig. 1 is inverted (viz. $f(x) \rightarrow x(f)$) and the residual is reformulated as $\underline{\Theta}(\underline{\mathbf{c}}, \Omega)$. The periodic non-linear force becomes the independent variable while the periodic displacement is calculated from the inverted force-displacement relationship.

$$x(f) = f + \left(\frac{1-\beta}{2}\right)[|f - f_c| - |f + f_c|] \tag{11}$$

where $\beta = 1/\alpha$ and $f_c = \alpha x_c$. Taking periodic $\underline{f}$ as the main solution target, the Jacobian is redefined as,

$$\underline{\underline{\mathbf{J}}} = \frac{\partial \underline{\mathbf{\Theta}}}{\partial \underline{\mathbf{c}}} = \left[\left(\frac{\Omega}{\upsilon}\right)^2 \underline{\underline{\mathbf{\Delta}}}^2 + 2\varsigma\left(\frac{\Omega}{\upsilon}\right)\underline{\underline{\mathbf{\Delta}}}\right]\frac{\partial \underline{\mathbf{a}}}{\partial \underline{\mathbf{c}}} + \underline{\underline{\mathbf{EI}}} \tag{12}$$

Here, $\underline{\underline{\mathbf{EI}}}$ is an $(2N_n\upsilon+1) \times (2N_h\upsilon+1)$ identity matrix. In this way, we successfully convert the calculation of $\partial \underline{f}/\partial \underline{x}$ to $\partial \underline{x}/\partial \underline{f}$ by defining:

$$\frac{\partial \underline{\mathbf{a}}}{\partial \underline{\mathbf{c}}} = \underline{\underline{\mathbf{\Gamma}}}^{+}\frac{\partial \underline{x}}{\partial \underline{f}}\underline{\underline{\mathbf{\Gamma}}}. \tag{13}$$

3.2 Excitation perturbation for sub-harmonic calculation

To identify and then calculate a sub-harmonic resonance, Kim et al. [5] first ran the MBHM using $\upsilon = 1$ and noted whether there were any unstable harmonic regimes beyond primary resonance. Should there exist such an unstable region, a second frequency sweep with $\upsilon = 2$ can be used to calculate the second sub-harmonic resonance. However, the responses at sub-harmonic regime are typically very complex (and not well understood) and consequently the calculation is highly sensitive to the choice of initial guess of $\underline{\mathbf{a_0}}$. For example, an inappropriate $\underline{\mathbf{a_0}}$ can lead to the same results as $\upsilon = 1$ case thereby failing to latch onto the sub-harmonic branch. For this reason, this approach would involve a certain amount of trial and error work to find a proper initial guess of $\underline{\mathbf{a}}$ and thus we refer to this as the initial guess approach.

To overcome the above-mentioned difficulty, we propose a new excitation perturbation method in this study. Namely, a perturbation item is to be artificially included in the excitation. For example, for the υth sub-harmonics, we write the input excitation as:

$$F(\tau) = F_m + \varepsilon_\upsilon \sin\left(\frac{\Omega}{\upsilon}\tau\right) + F_p \sin(\Omega\tau) \tag{14a}$$

Therefore for the 2nd-subharmonic,

$$\underline{\mathbf{Q}} = [F_m \quad \varepsilon \quad 0 \quad F_p \quad 0 \quad \cdots \quad 0]^T \tag{14b}$$

Note that the perturbation term ε shall be very small, for instance $\varepsilon = (10^{-4} - 10^{-3})F_p$. A higher value of ε is not recommended as it would couple the non-linear sub-harmonic response and the linear response excited by the second harmonic term. With this perturbation item, the sub-harmonic resonance can be effectively triggered and the sensitivity of initial guess as experienced in the aforementioned conventional approach is remarkably reduced. Consequently, the sub-harmonics could be calculated with just one run of frequency sweep. Also, the initial guess is not a serious issue for our approach as long as Ω_0 is reasonably far away from the primary resonance whose upper limit (assuming the system always operates within the stiff stage) can be easily defined as $\mathbf{max}(\Omega_{prim}) = \sqrt{\alpha}$. Another scenario that requires careful treatment is when an isolated sub-harmonic branch would occur, as we will discuss later. Figure 2 compares the results of initial guess approach, excitation perturbation approach and a numerical integration scheme using Runge-Kutta with adaptive size control [8]. Excellent agreement is clearly observed between these three approaches. Note that the excitation perturbation approach takes only one run to complete the response characteristics.

4 Results and discussion

For clearance type non-linearity where $\alpha \in [0, 1)$, Kim et al. found that the crossing of mean operating point from the stiff to the compliant stage plays an important role [5]. For instance, they found a 2nd sub-harmonic resonance occurs when the separation between the crossing point Ω_c and primary resonance Ω_p is sufficiently far, i.e. $(\Omega_c - \Omega_p) > \Omega_p$. Following this criterion, they stated if the mean operating point $x_m(\Omega)$ always staying within the compliant stage and thus $(\Omega_c - \Omega_p) = \infty$, then a sub-harmonic resonance could exist. But, as evident from Fig. 3, this criterion no longer holds for the case when $\alpha > 1$. Following their

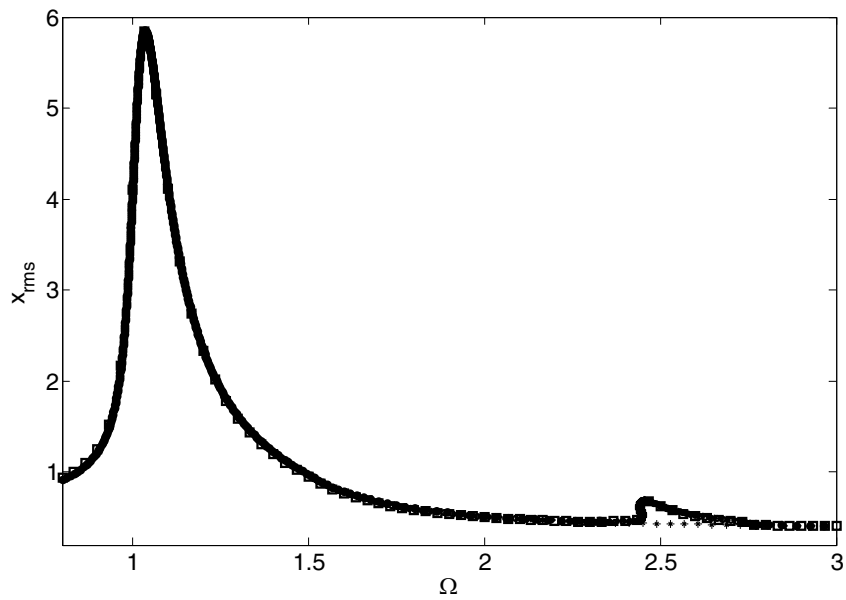

(a)

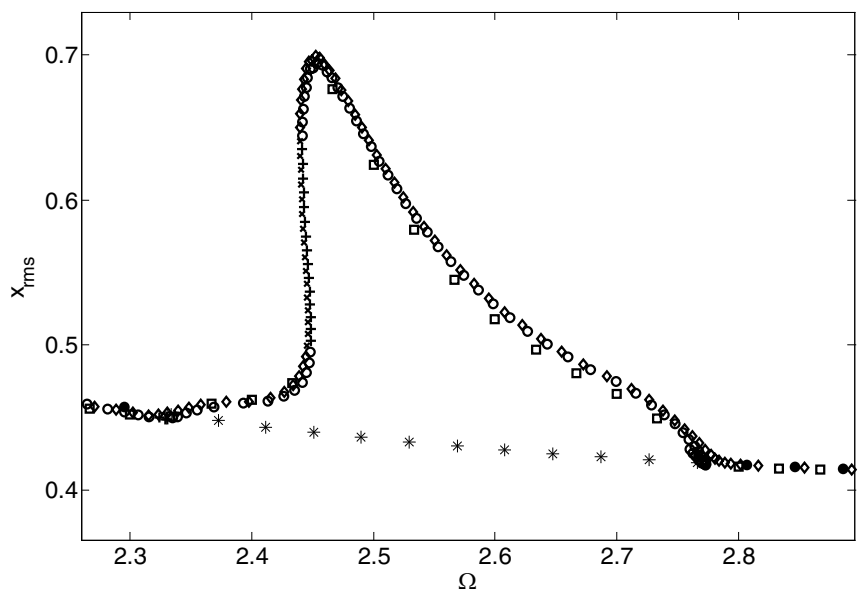

(b)

Fig. 2 Comparison of Calculation Results, given $\alpha = 2$, $\varsigma = 0.05$, $F_{\mathrm{m}} = 0.80$ and $F_{\mathrm{p}} = 0.85$. (a) Primary and Sub-harmonic Resonances. (b) Enlarged View of Sub-harmonic Resonance. Key: ●●●: stable solution of MHBM first run; ∗∗∗, unstable solution of MHBM first run; ○○○: stable solution of initial guess approach with MHBM second run; + + +: Unstable solution of initial guess approach with MHBM second run; ◊◊◊: stable solution of excitation perturbation approach; × × ×: unstable solution f excitation perturbation approach; □□□: numerical integration with Runge-Kutta scheme

initial guess approach and running the MHBM with $\upsilon = 2$, a sub-harmonic resonant peak is clearly seen in Fig. 3 but $(\Omega_{\mathrm{c}} - \Omega_{\mathrm{p}}) < \Omega_{\mathrm{p}}$. Note that $x_{\max}$, x_{m} and $x_{\min}$ stand for maximum, mean and minimum responses respectively at each Ω. As indicated by x_{m}, the system behaves nonlinearly in the primary resonance regime, and there is "dynamic" crossover between the first and second stage. In such case, the primary resonant frequency is a combined effect of the stiff first stage and the compliant second stage. Consequently, the system shows softening characteristics and the resultant Ω_{p} is lower than $\sqrt{\alpha}$.

To study the occurrence of sub-harmonic resonance, parametric study is conducted. For the dimensionless system of Equation (4), F_{m}, F_{p} and α can sufficiently describe the system, assuming a light damping ratio of

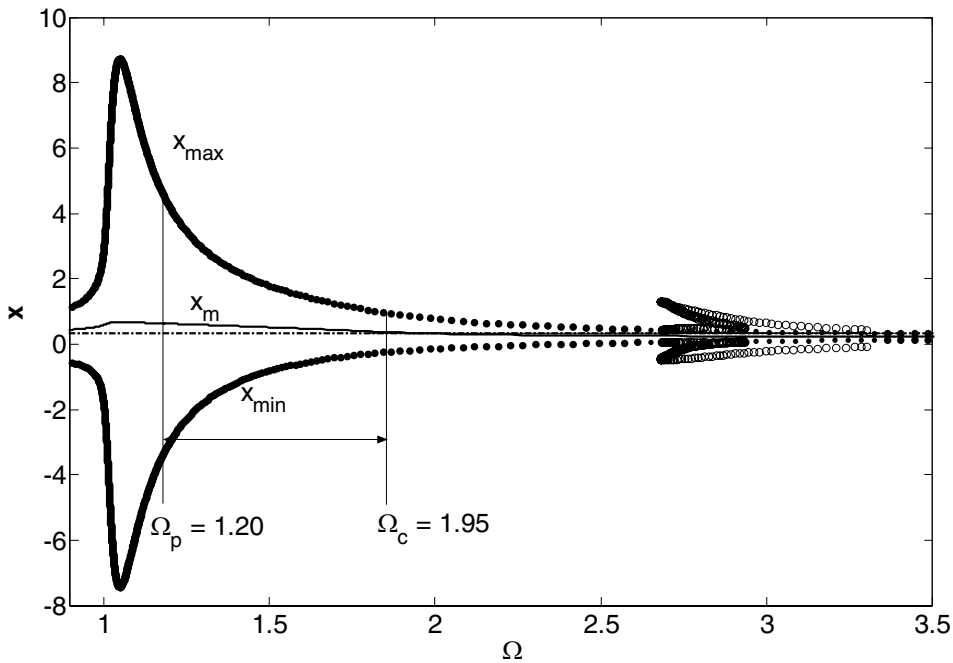

Fig. 3 Sub-harmonic Resonance given $\alpha = 3$, $\varsigma = 0.05$, $F_{\mathrm{m}} = 0.70$ and $F_{\mathrm{p}} = 0.85$. Key: ●●●, MHBM result with $\upsilon = 1$; ○○○, MHBM initial guess approach with $\upsilon = 2$; $- \cdot -$, transition point value; —, mean operation $x_{\mathrm{m}}(\Omega)$

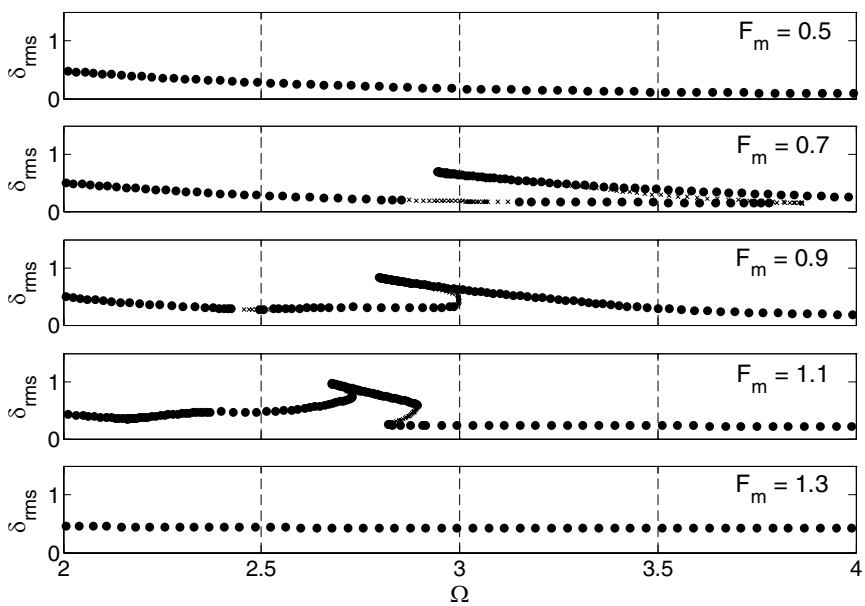

Fig. 4 Effect of F_{m} on the occurrence of sub-resonance given $\alpha = 8$ and $F_{\mathrm{p}} = 0.75$. Key: ●●●, stable response; ×××, unstable response

$\varsigma = 0.05$. First, we study the effect of F_{m} on the sub-harmonic resonance. In Fig. 4, when F_{m} starts from 0.5, no sub-harmonic resonance is found. As F_{m} moves closer to the transition point (viz. $F_{\mathrm{m}} = 1.0$), for example $F_{\mathrm{m}} = 0.7, 0.9$, a 2nd sub-harmonic resonance is clearly observed. Also, a 2nd sub-harmonic resonance occurs even when the starting mean operating point x_{m0} is close enough to the transition point, for example, $F_{\mathrm{m}} = 1.1$. Here x_{m0} is defined as follows:

$$x_{m0} = \begin{cases} F_{\mathrm{m}}/\alpha & F_{\mathrm{m}} \leq 1.0 \\ F_{\mathrm{m}} + \frac{1.0-\alpha}{\alpha} & F_{\mathrm{m}} > 1.0 \end{cases} \tag{15}$$

Note that we focus on the positive definite mean load cases in this article. Since the non-linear force-displacement relationship is an odd function as shown in Fig. 1, the system dynamics for a negative mean load could be symmetrically mapped. In the extreme case when $F_m = 1.0$, even a small excitation F_p will generate sub-harmonic resonance. For example in Fig. 5, an active 2nd sub-harmonic peak occurs although F_p is as small as 0.01. Further, it is noted that the sub-harmonic peak frequency decreases with an increase of F_m. For example, as F_m increases from 0.7 to 1.1, the sub-harmonic peak frequency decreases from

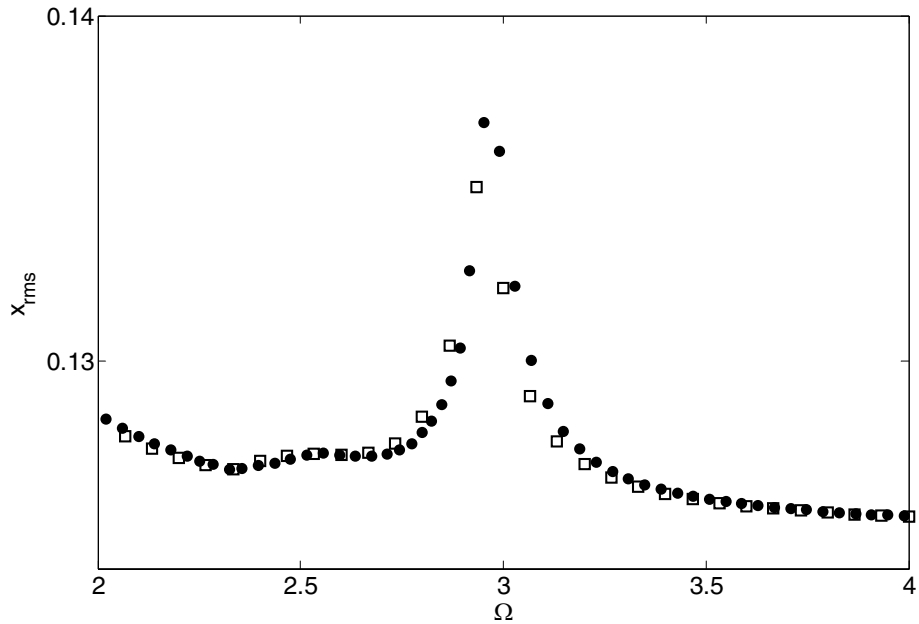

Fig. 5 Sub-harmonic Resonance when $F_m = 1.0$ given $\alpha = 8$ and $F_p = 0.01$. Key: ●●●, MHBM result; □□□, Numerical integration result

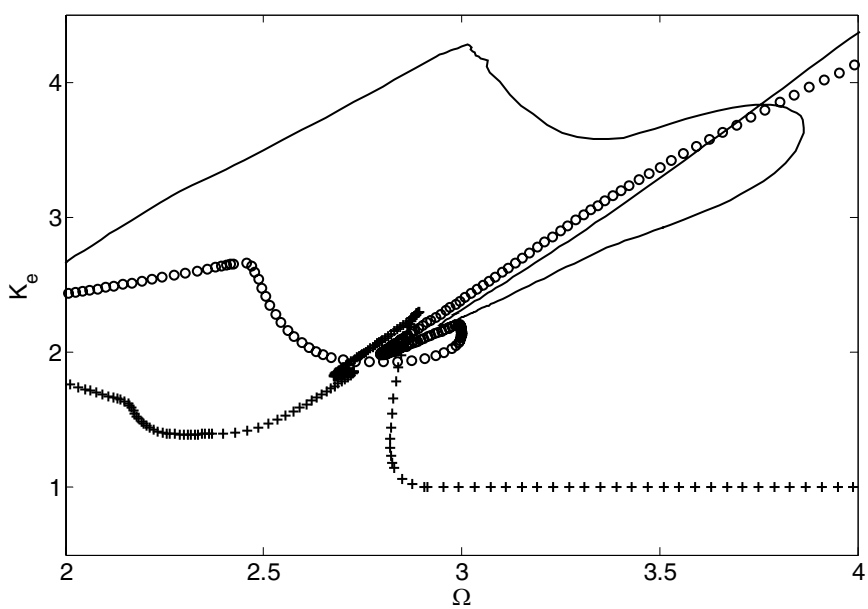

Fig. 6 Comparison of Equivalent Stiffness. Key: —, $F_m = 0.7$; ○○○, $F_m = 0.9$; + + +, $F_m = 1.1$

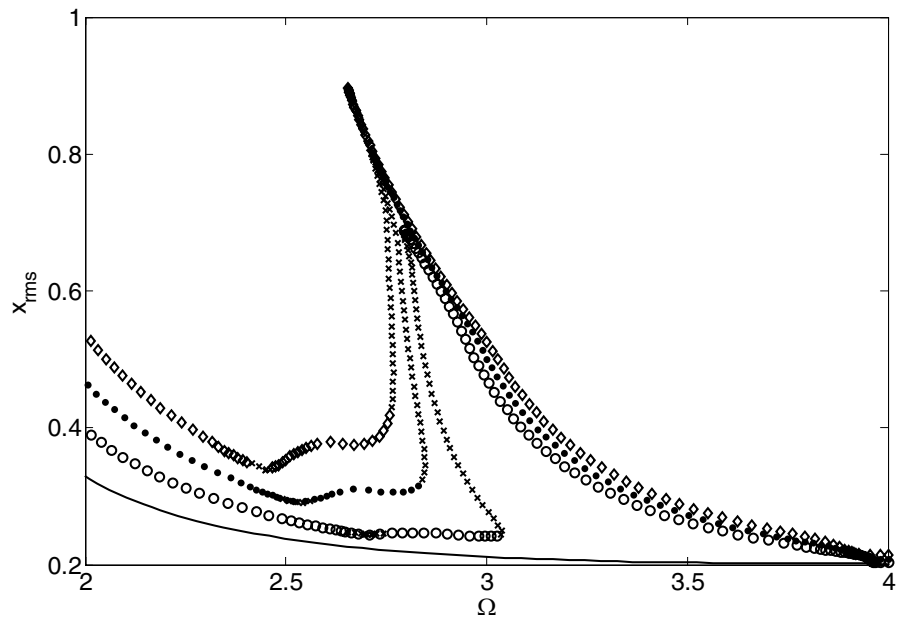

(a)

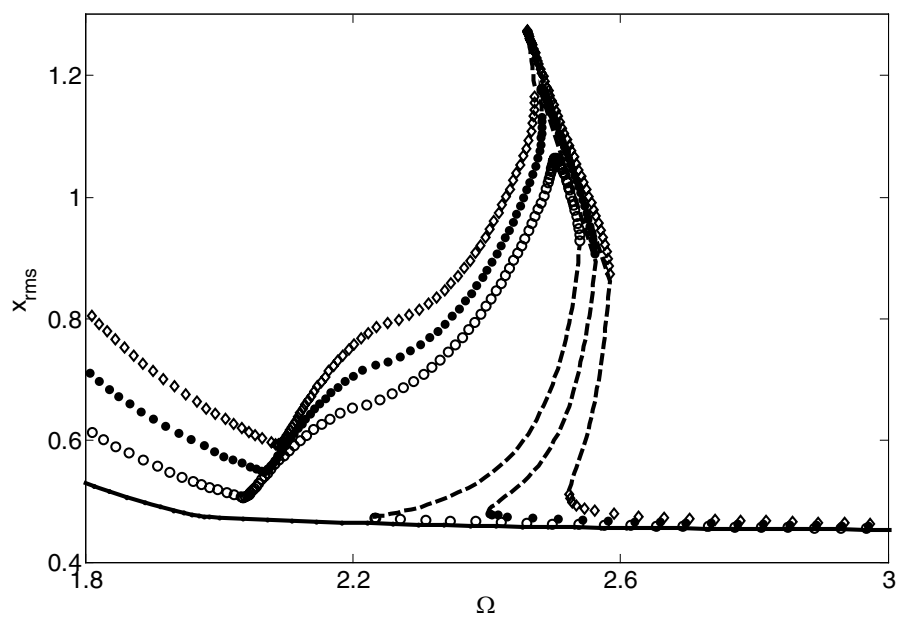

(b)

Fig. 7 Effect of F_p on Sub-harmonic Resonance given $\alpha = 4$. (a) For $F_m = 0.80$. Key: —, $F_p = 0.4$; ○○○, $F_p = 0.6$; ●●●, $F_p = 0.8$; ◇◇◇, $F_p = 1.0$, − − −, unstable solutions. (b) For $F_m = 1.20$. Key: —, $F_p = 0.6$; ○○○, $F_p = 0.8$; ●●●, $F_p = 1.0$; ◇◇◇, $F_p = 1.2$, − − −, unstable solutions

$\Omega = 2.95$ to 2.68. This could be explained by an effective stiffness K_e concept.

$$K_e = \frac{\frac{1}{N-1}\sum_0^{N-1}(f(x) - \langle f(x)\rangle_N)(x - \langle x\rangle_N)}{\frac{1}{N-1}\sum_0^{N-1}(x - \langle x\rangle_N)(x - \langle x\rangle_N)} \quad (16)$$

Here $\langle\ \rangle_N$ is the arithmetic average of N discrete points calculated by MHBM. As presented in (16), this is indeed an unbiased covariance calculation [10]. Figure 6 compares K_e of three F_m in the sub-harmonic resonance regime. As seen, a higher F_m generally has lower K_e in the sub-harmonic resonant regime. Note that the

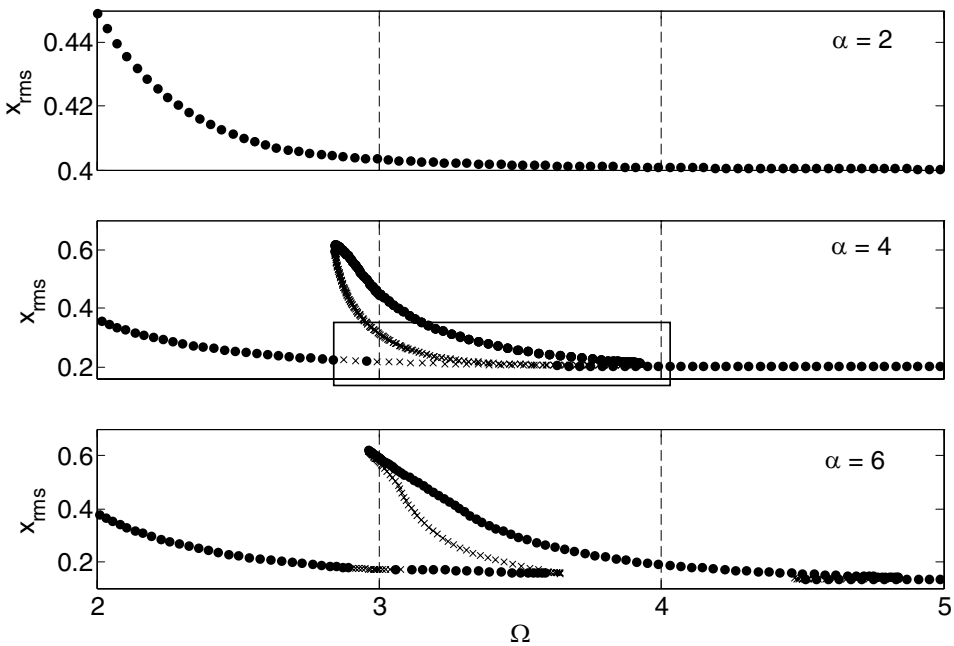

(a)

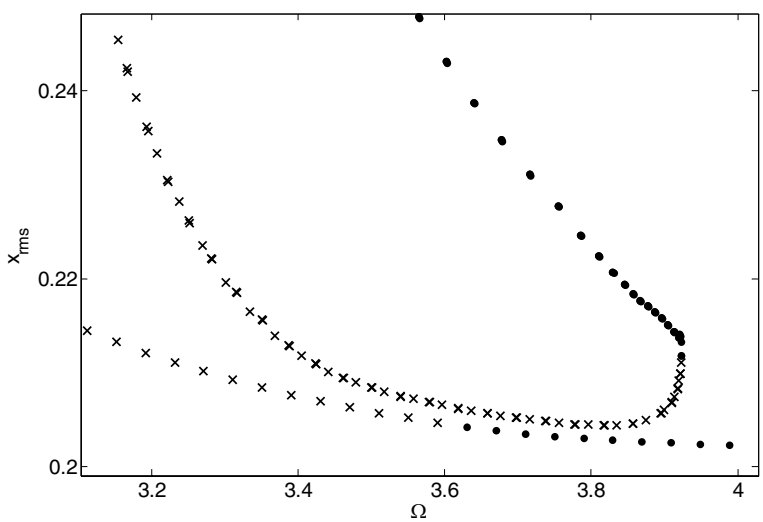

(b)

Fig. 8 Effect of α on Sub-harmonic Resonance given $F_m = 0.80$ and $F_p = 0.50$. (a) Frequency responses. (b) Enlarged view of isolated branch. Key: ●●●, stable solution; ×××, unstable solution

resonant peak response is actually a joint effect of the whole regime rather than K_e at a specific Ω. For this reason, although at some frequencies the effective stiffness K_e (with higher F_m) is larger than that for lower F_m, the overall effect across the frequency range yields a lower peak frequency. Physically, with lower F_m, system operates more in the first stage with higher stiffness that results in a higher sub-harmonic resonant peak frequency.

Next, the effect of F_p is investigated. Figure 7a shows the results when x_{m0} stays in the first (stiffer) stage ($F_m < 1$) and 7b in the second (compliant) stage ($F_m > 1$). As is shown, in both cases as F_p increases, the root-mean-square response also increases as a result of enhanced excitation. In either case, there is a slightly downshifting of peak frequency as F_p increases. Though the calculation of K_e would help in examining this frequency shifting phenomena, similar to the previous discussion, we provide an intuitive yet sensible explanation here. Although an increase of F_p is symmetric around F_m and thus x_{m0} in terms of excitation force, the asymmetric nature of the piecewise linear system introduces different duty-cycles of stiffer and compliant stages. As a matter of fact, the periodic response of piecewise linear system is a combination of two transient responses within stiff and compliant stages, referring to the piecewise solution strategy [9]. Theoretically, the higher the stiffness (or frequency) is, the shorter the response (decay) time is. Consequently, although an increase in the dynamic excitation F_p is symmetric around F_m, the enhanced response is not symmetric as a result of the asymmetric non-linearity. Thus, the proportion of time that the system operates within the stiff stage shall be smaller than in the compliant side within one period of response. Therefore an increase in F_p would decrease the peak frequency.

Finally, we examine the effect of α value. Figure 8 shows a cascading plot of frequency response in the sub-harmonic resonance regime. It is evident that the sub-harmonic tends to take place with an increase in α. It is because when α is higher, the transition point $1.0/\alpha$ is smaller. Further, a higher stiffness would enlarge the dynamic response (as contributed by F_p) at higher frequency. Therefore, it is easier for the system to go through the transition point. Since such transition indicates a switch from linear to nonlinear system behavior, a higher transition frequency would introduce more complicated system dynamics such as sub-harmonic resonance. Further, it is noted that as sub-harmonic resonance first appears when $\alpha = 4$, an isolated closed-loop sub-harmonic branch is found. Because the system initiates in the first (stiffer) stage ($F_m < 1$), the system trends to soften up as it moves in the second region; hence the resonance branch in Fig. 8a tilts to the left. As discussed earlier in Section 3, the excitation perturbation approach cannot be directly applied in this

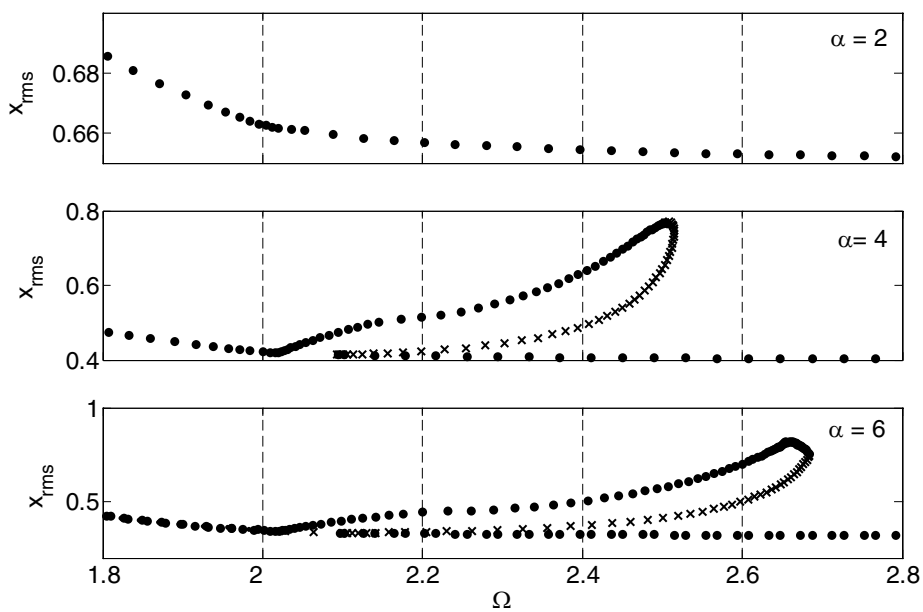

Fig. 9 Effect of α on Sub-harmonic Resonance given $F_m = 1.15$ and $F_p = 0.50$. Key: ●●●, stable solution; ×××, unstable solution

case. As shown in Fig. 8b, the closed-loop branch is totally isolated from the lower locus. The excitation perturbation approach, taking the adjacent points as initial guess for next calculation, cannot take the jump. Rather, the initial guess approach must be used by taking a trial and error process to find the appropriate initial conditions. Figure 9 also shows a similar trend: a higher α would bring sub-harmonic resonance more easily. Because the system initiates within the second (compliant) stage ($F_m > 1$), the system stiffens up as it expands into the first region; hence the resonance branch in Fig. 9 tilts to the right, typical for a hardening nonlinearity.

5 Conclusion

In this study, we studied the sub-harmonic resonance of a mechanical oscillator with a nearly pre-loaded non-linearity. Several contributions to the state-of-art emerge. First, with a new excitation perturbation approach, we have successfully applied MHBM to calculate the sub-harmonic resonances. Our approach has significantly reduced the work by computing the sub-harmonic responses with just one run. Initial guesses in the vicinity of sub-harmonic regime are relaxed compared to previous approach. Second, effects of F_m, F_p and α on the occurrence and characteristics of sub-harmonic resonances have been examined. Our analysis shows that the sub-harmonic resonance typically happens when F_m is close to the transition point. In the extreme case, a very small F_p would be sufficient to excite a sub-harmonic resonance. For a higher F_m, the resonant peak appears in lower frequency as a result of reduced equivalent stiffness. The possibility of the sub-harmonic occurrence also increases as an increase of F_p or α. Finally our analytical formulations have been validated using numerical integration results. Future work would focus on analytical study of sub-harmonic resonances in multi-degree of freedom systems with preload type nonlinearity.

Appendix A: List of symbols

C	viscous damping coefficient
F	force
M	mass
N	number of integration points
K	stiffness
t	time
x	displacement
ω	excitation frequency (rad/s)
ε	perturbation
Ω	dimensionless frequency
τ	dimensionless time
ζ	damping ratio
Δ	differential operator matrix
Γ	discrete Fourier transform matrix
Subscripts	
c	crossing
e	equivalent
m	mean load
n	natural frequency or index
p	fluctuating component or primary
0	initial or starting
Superscripts	
-	dimensional variable or parameter
$'$	first derivative with respect to dimensionless time
$''$	second derivative with respect to dimensionless time
-1	inverse
$+$	pseudo inverse
T	transpose
Operator	
$\langle\ \rangle$	arithmetic averaging

References

1. Comparin, R.J., Singh, R.: Nonlinear frequency response characteristics of an impact pair. J. Sound Vib. **134**(2), 19–40 (1989)
2. Choi, H.S., Lou, J.Y.K.: Nonlinear behavior and chaotic motions of an SDOF system with piecewise non-linear stiffness. Int. J. Non-Linear Mech. **26**, 461–473 (1991)
3. Padmanabhan, C., Singh, R.: Dynamics of a piecewise nonlinear system subject to dual harmonic excitation using parametric continuation. J. Sound Vib. **184**(5), 767–799 (1995)
4. Padmanabhan, C., Singh, R.: Analysis of periodically forced non-linear Hill's oscillator with application to a Geared system. J. Acoust. Soc. Am. **99**(1), 324–334 (1996)
5. Kim, T.C., Rook, T.E., Singh, R.: Super- and sub-harmonic response calculations for a torsional system with clearance non-linearity using harmonic balance method. J. Sound Vib. **281**(3–5), 965–993 (2005)
6. Duan, C., Singh, R.: Dynamic analysis of preload nonlinearity in a mechanical oscillator. J. Sound Vib. (accepted for publication) (2006)

7. Gelb, A., Vander Velde, W.E.: Multiple-Input Describing Functions and Non-linear System Design. McGraw-Hill, New York, USA (1968)
8. Dormand, J.R., Prince, P.J.: A family of embedded Runge–Kutta formulae. J. Comput. Appl. Math. **6**(1), 19–26 (1980)
9. Duan, C., Singh, R.: Dynamics of a 3DOF torsional system with a dry friction controlled path. J. Sound Vib. **289**(4–5), 657–688 (2006)
10. Rook, T.E., Singh, R.: Dynamic analysis of a reverse – idler gear pair with concurrent clearances. J. Sound Vib. **182**(2), 303–322 (1995)